Energy Technology
Generation, Conversion, Storage, Distribution
www.entechnol.de

A New Anion Exchange Membranes Pretreatment Protocol for Hydrogen Production by Water Electrolysis

Manuel Ángel González Rodríguez, Cirilo Delgado, Abiodun Abiola, José Manuel Andújar, and Francisca Segura**

This study examines the impact of pretreatment techniques on anion exchange membrane (AEM) used in water electrolysis for hydrogen production. A new pretreatment protocol is proposed, involving membrane immersion in Milli-Q water for 7 days and 8 h conditioning in the electrolytic stack. The new pretreatment protocol is compared with three conventional protocols, based on short-term exposure to alkaline electrolytes (0.1 M KOH). Morphological analysis using scanning electron microscopy-energy-dispersive X-ray detector and electrochemical performance evaluation through polarization curves are conducted. Results show that the new pretreatment protocol improves hydrogen production efficiency by 2.6% compared to conventional alkaline pretreatments. This improvement is resulting of an increase in membrane hydration during the pretreatment, which benefits the ion-exchange process during the 8 h conditioning, reducing chlorine ion content from 0.2% to 0.1%. Tafel slope analysis further supports these findings. These study highlights the need for further research on AEM pretreatment protocols to optimise hydrogen production by electrolysis performance, reduce the use of reagents and mitigate the effects of long-term degradation of membranes.

1. Introduction

The serious climate crisis that global society is suffering, motivates the actual research on low emissions hydrogen as energy vector. To obtain low emissions hydrogen, water electrolysis becomes one of the most promising technologies. In this sense, water electrolysis can be classified on two groups: low temperature (<90 °C) and high temperature (>1000 °C). Inside low temperature group, alkaline electrolysis (AE), and proton exchange membrane (PEM) are two commercially available technologies. **Figure 1**a,b show operating principles of these electrolysis technologies. Nevertheless, there is currently a great interest in alternative electrolysis systems based on the use of anion exchange membranes (AEM). AEM technology, Figure 1c, combines features from both, AE and PEM electrolysis, using alkaline environments and exchange membranes. That is, AEM technology requires lower alkaline concentrations (0.1–1% KOH) than AE, it does not require high water purity as PEM technology (conductivity <50 μS cm^{-1} in case of PEM electrolysers) and operating conditions can be optimised to avoid the use of precious catalysts.[1,2] Due to potential AEM technology advantages over AE and PEM, recent research focuses on improving the operation of AEM electrolysers to achieve higher current density values.

This study analyses the impact of pretreatment techniques on AEM. For this purpose, a new pretreatment protocol is proposed, based on using Milli-Q water, mitigating the use of reagents and reducing the effects of long-term degradation of membranes. The main novelty of the research is that it integrates morphological, compositional, and electrical performance analyses to evaluate the pretreated membranes, considering not only their chemical composition but also their interaction with the complete electrolyte system.

Regarding recent scientific literature, other studies provide valuable insights into the design,[3] operation,[4–6] and optimisation[7,8] of AEM electrolysis systems. The authors' research distinguishes itself by providing an in-depth and structured analysis of how pretreatment techniques affect membranes, supported by an experimental methodology that allows correlating these modifications with their electrochemical performance. **Table 1** shows the main contributions of this study in comparison to the scientific literature, both from the research sector and private companies. The classification has been made according to the key contributions and the content related to the additional contributions and discoveries of this detailed study.

2. Experimental Section

For the experimental development, four different pretreatment protocols are conducted on AEM membrane: protocol a) a

M. Á. González Rodríguez, C. Delgado, A. Abiola, J. M. Andújar, F. Segura
Research Centre on Technology
Energy and Sustainability (CITES)
University of Huelva
Campus El Camen, 21071 Huelva, Spain
E-mail: manuelangel.gonzalez@diesia.uhu.es;
francisca.segura@diesia.uhu.es

The ORCID identification number(s) for the author(s) of this article can be found under https://doi.org/10.1002/ente.202500249.

DOI: 10.1002/ente.202500249

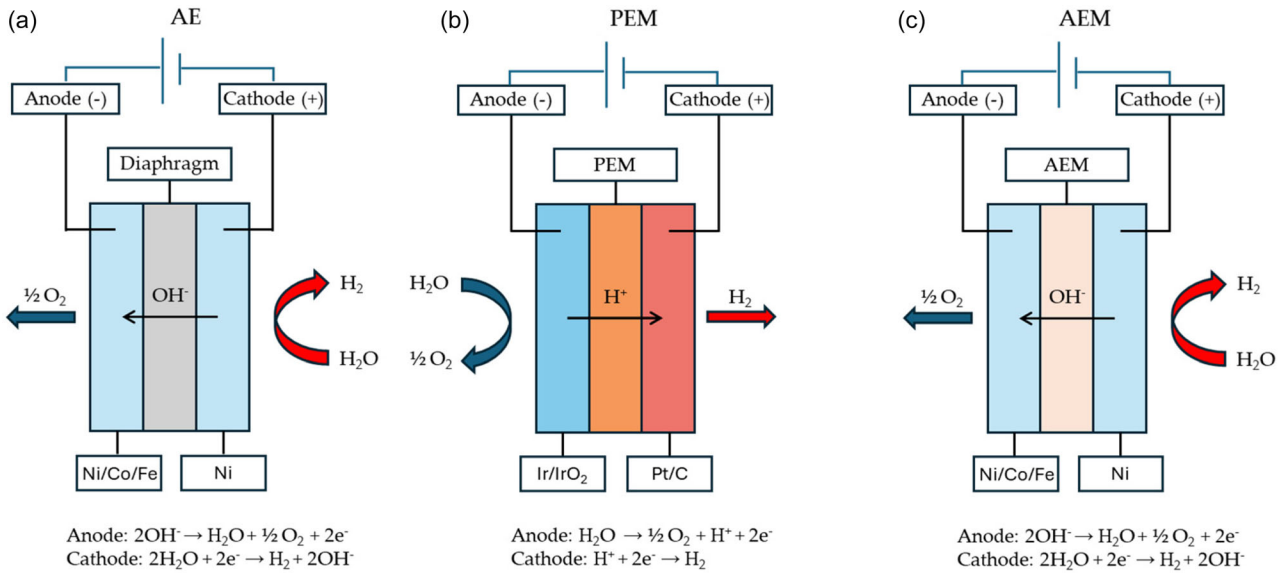

Figure 1. Operational principle of a single cell in electrolysis technologies: a) AE, b) PEM, and c) AEM.[2]

Table 1. Authors' contributions and related studies.

Scientific studies	Key contributions	Pretreatment study	SEM-EDX study
Authors' Proposal	Development of a new pretreatment protocol for anion exchange membranes	Immerse the membrane for 7 days in Milli-Q water and subsequent conditioning for 8 h inside an AEM electrolyser. The results are compared with commercial pretreatment protocols and the pretreatment conditions are justified.	Morphological and compositional study of the surface of AEMs.
[3]	Review of the state of the art of AEM electrolysis technology, identifying gaps and making recommendations for research focused on this technology.	Immerse the membrane overnight in 1 M $KHCO_3$ and then cleaning it with water to remove any residues. This review does not make a comparative study of different pretreatment protocols, does not justify the pretreatment conditions and has a negative environmental impact.	n/a
[4–6]	Study of operating conditions and the use of catalysts to improve the efficiency of the AEM electrolysis process.	Highlight the importance of carrying out membrane pretreatment under appropriate conditions, as this is a factor influencing the electrolysis process. This study does not explain the pretreatment conditions.	Only Xu et al.[14] carry on a morphological study of AEMs.
[7]	Investigate the effect of KOH electrolyte addition on the performance of AEM electrolysers.	Immerse the membrane in a 1% KOH aqueous solution for 4 h at room temperature. This study justifies the pretreatment conditions but has an associated reagent cost and environmental impact.	n/a
[8]	Development of a blending technique to synthesize AEMs with lower ion migration resistance and better performance.	Immerse the membrane in a 1 M KOH aqueous solution for 48 h at room temperature. This study justifies the pretreatment conditions but has an associated reagent cost and environmental impact.	Morphological study of the surface of AEMs.

To carry out the study, the article is organized as follows: Section 2 describes materials and method used in the pretreatment protocols preparation. Section 3 presents the new pretreatment protocol proposed by authors, and the experimental results are shown in Section 4. Finally, Section 5 and 6 summarize main discussions and conclusion of the research.

non-pretreated membrane to see the effects of not applying pretreatment; protocol b) manufacturer's pretreatment protocol; protocol c) modified manufacturer's pretreatment protocol; and protocol d) pretreatment protocol proposed by authors.

Section 2.1 describes the main characteristics of the membrane and Section 2.2 defines the methodology used in the research.

2.1. Membrane Fundamental Characteristics

Membranes used in AEM electrolysis are made of polymeric carbon networks in which functional groups are grafted, allowing hydroxyl groups to be exchanged. Depending on the manufacturer, the composition of the AEM membranes changes and therefore the current density values that can be

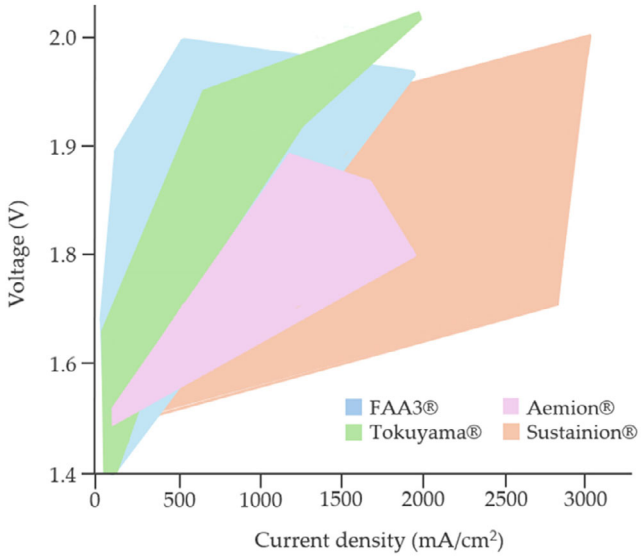

Figure 2. Theoretical voltage (V) versus current density (mA·cm^{-2}) curves of different types of AEM membranes.[1]

reached at a certain voltage are also affected. **Figure 2** illustrates the theoretical performance of AEM membranes available on the market.[9–11]

The voltage versus current density curves obtained from each membrane manufacturer are different because the chemical composition of the membrane plays a fundamental role in the ion-exchange process during the electrochemical reaction. In this case study, authors have used Tokuyama membrane (model A210). Tokuyama's membranes are characterised by a high stability under AEM electrolysis operating conditions, together with a low water absorption capacity (around 25%). This is an important property, because the degradation rate of the membrane is very low, about 10 μV h^{-1} over 5000 h.[12] Membrame model A210 is not commercial, but its chemical structure is similar to commercial model A201. It is composed of a hydrocarbon polymer backbone with quaternary ammonium groups linked by electrostatic interactions with chloride ions. The quaternary ammonium groups are responsible for the ionic-exchange process of the membrane. Initially, the membrane in its dry form has these groups linked with chloride ions. When the pretreatment and conditioning of the membrane are carried out, it hydrates due to the action of water and undergoes an exchange process of these chloride ions, which is transferred to the medium that has been used for pretreatment while the membrane becomes loaded with hydroxyl groups.[13–15]

2.2. Methodology

Once the membrane has been selected, it is necessary to use an appropriate pretreatment protocol due to electrochemical behaviour depends deeply on the process followed to activate the membrane. If the membrane has been correctly hydrated, its internal channels open more, allowing a greater flow of ions. This enhances the ion conductivity between the two sites of the membrane. Therefore, a good ion exchange between chloride ions and hydroxyl groups must be achieved to generate more active sites in the membrane.[16] After pretreatment, scanning electron microscopy (SEM)-energy-dispersive X-ray detector (EDX) analysis will be carried out to determine the structure and chemical composition of membranes pretreated under different protocols, relating it directly to its efficiency in the electrolysis stack. The efficiency will be quantified by polarization curves and will be corroborated determining the Tafel slopes.

The methodology followed by authors, to carry out the study of pretreatment effects on AEM membranes, consists of four stages (**Figure 3**): 1) Membrane cutting; 2) pretreatment; 3) SEM-EDX analysis, and 4) electrochemical performance analysis, operation, and polarization V–I curve.

As summary, **Table 2** shows all the materials and equipment used in each of the points of this research to cut the Tokuyama membranes (1), to carry out the pretreatment of the membranes (2), to characterise the membranes by SEM-EDX (3) and to study the performance and VI curve (4).

3. New Pretreatment Protocol

Considering the basic structure of an AEM electrolytic single-cell stack, **Figure 4**, it operates in alkaline environments, featured with a membrane that allows hydroxyl ions generated in the cathode compartment to move toward the anode.[1,2]

3.1. Laser Cutting

The first step is to cut the Tokuyama A210 membranes to the appropriate diameter to insert it into the single-cell stack. The membrane is cut with a diameter of 100 mm and it has a thickness of 28 μm. To cut the membranes, a laser cutting machine model USB690g Cabinet Laser Engraver is used. The cutting conditions were optimised to achieve a precise cut without

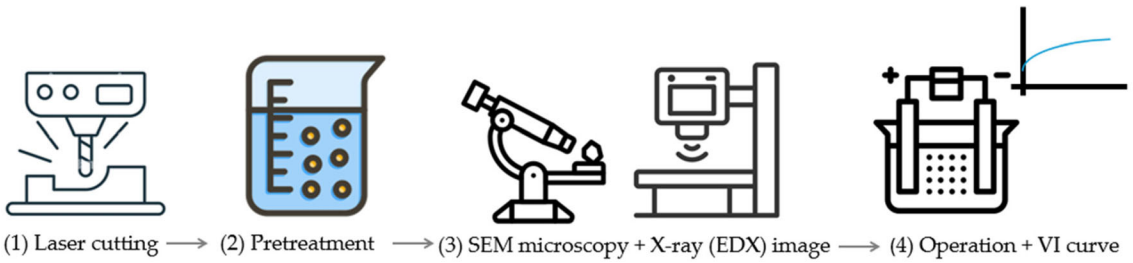

Figure 3. Stages of the research to study the effects of the pretreatment in AEM membranes.

Table 2. Technical data of equipment used by authors in the research.

Stages	Technical data
1) Laser cutting	Model USB690g Cabinet Laser Engraves Parameters: Laser Tube: CO, Laser Wavelength: 10640 nm, Diameter Length: 2.4 in and Max. Processing Speed: 8000 mm s^{-2}
2) Pretreatment	400 mL beakers, Kenzium 1000 mL volumetric flask, Simax Magnetic stirrer, Anzeser ($\omega = 0$–3500 rpm) Analytical laboratory balance, WELLiSH (max = 2000 g, d = 0.01 g) Potassium hydroxide, KOH, Alquera, p.a = 90% Milli-Q water, HYDROLAB ($\rho = 18.2\ \mu\Omega$ cm) AEM membrane A210 from Tokuyama
3) SEM-EDX image	Model: JEOL-JSM 5410 and EDX Oxford ISIS-Link Parameters: Tungsten electron source, a magnification range of 18*x* to 300,000*x*, and a maximum resolution of 3.5 nm
4) Operation and VI curve	AEM stack (in-house manufacturing), cell active area Ø10 cm Arduino controller: NI USB 6002 Flow controller: Model ABB ACS355 Peristaltic pump: Tapflo - PT10 GR-05/43 Volumetric flask: Volume = 1000 mL, Borosilicate Glass, Simax Electronic heater: Rate power = 1500 W and Material = Stainless Steel Power supply: Newpower, Rate power = 3000 W, Output = 0.1–100 A Temperature controller: STC 1000, Range = −50–99 °C, Resolution = 0.1 °C and Accuracy ± 1 °C

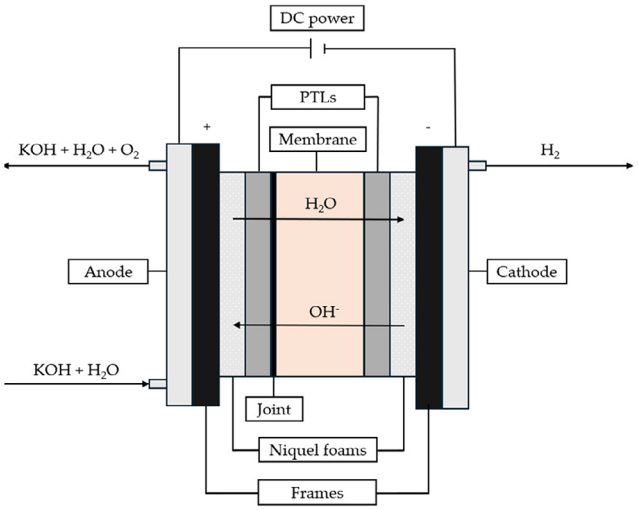

Anode half-reaction: $2\ OH^- \longleftrightarrow H_2O + 1/2\ O_2 + 2\ e^-$ $E_0 = 0.401$ V

Cathode half-reaction: $2\ H_2O + 2\ e^- \longleftrightarrow H_2 + 2\ OH^-$ $E_0 = -0.828$ V

Overall reaction: $H_2O \longleftrightarrow H_2 + 1/2\ O_2$ $E_0 = 1.23$ V

Figure 4. Scheme of an AEM electrolytic single-cell stack and chemical reactions of each half-cell.[4]

burning the membrane surface. The three cutting parameters that can be configured are: power, speed and passes. **Table 3** compiles the tested configurations. Of all the configurations tested, configuration 3 is the most suitable, as the cut was precise and without burns.

Table 3. Parameters configuration for USB690g cabinet Laser engraves.

Configuration	Power [%]	Speed [mm sec^{-1}]	Passes
1	20	70	1
2	15	80	1
3	12	100	2

3.2. Pretreatment

To study the effects of different pretreatments in AEM membranes, authors have defined three pretreatment protocols, over the basis of a non-pretreated membrane. All tests were carried out under normal temperature and pressure conditions (NTP), and with a relative humidity (RH) in the environment between 60 and 70%. The first protocol, **Figure 5**a, proposes to use the membrane without pretreatment. The membrane without pretreatment will be stored for analysis via SEM-EDX, and after this analysis, the membrane will be operated into the test bench.

The second protocol, Figure 5b, is based on membrane manufacturer recommendation: immersing the membrane into 0.1 M KOH electrolyte solution during 30 min, in three separated containers, and at the end, the membrane is cleaned with Milli-Q water, to remove the surplus electrolyte solution.

The third protocol, Figure 5c, is a modification from manufacturer's procedure. The immersion time is reduced to 20 min, but the number of immersions is increased up to four. In this case, the membrane is not cleaned with Milli-Q water after the pretreatment.

Finally, protocol proposed by authors, Figure 5d, consists on pretreating the membrane in Milli-Q water for 7 days and conditioning it for 8 h inside the AEM single-cell stack. It is necessary to carry out the pretreatment for 7 days because this long period of time helps to

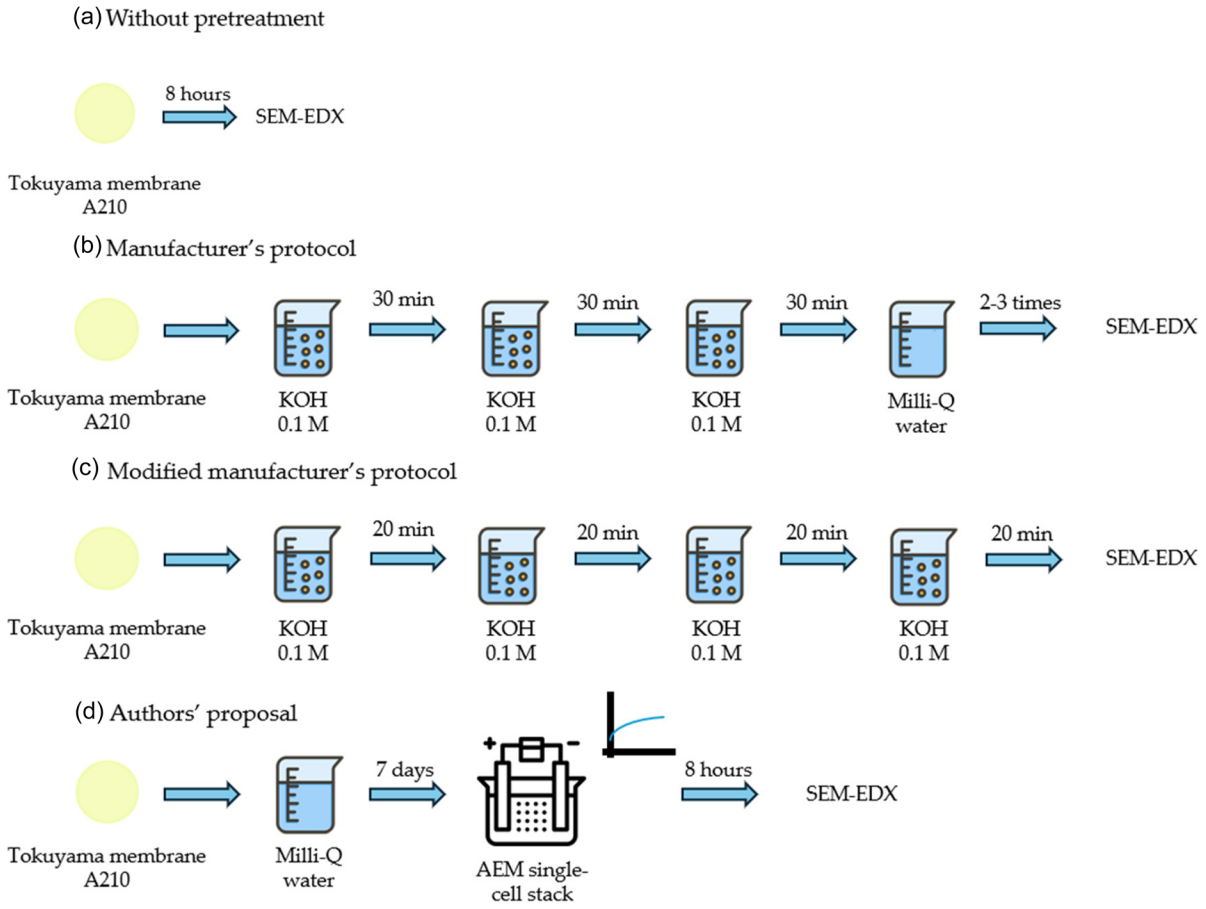

Figure 5. Pretreatment techniques used during the study: a) Without pretreatment, b) Manufacturer's protocol, c) Modified manufacturer's protocol, and d) Authors' proposal.

open the internal channels of the membrane, which improves its electrochemical performance because the membrane reaches a high degree of hydration.[17] In addition, using Milli-Q water prevents the degradation of the membrane's chemical structure, which would occur if it were pretreated with KOH 0.1 M during the same period, due to the degradation of the membrane's polymer backbone.[1,2,18] Subsequently, conditioning the membrane for 8 h inside the AEM single-cell stack allows the ion exchange between the chloride ions of the membrane and the hydroxyl groups of the electrolyte. Due to the opening of the channels achieved by pretreating the membrane in Milli-Q water for 7 days, the ion-exchange process is enhanced. Once the protocol has been completed, if no further analysis of the membrane is required, the membrane can be kept in the AEM single-cell stack, and the electrolyte can be recirculated. However, it is important to include a chloride ion exchange filter on the test bench to retain these ions, preventing the chloride ions that have passed into the medium from accumulating.

3.3. SEM-EDX Image

To analyse the effect of the different pretreatment protocols, the SEM technique will be used, as it allows the study of the morphology of the membrane surface. Additionally, X-rays image (EDX) allows to identify the elemental composition of the membrane surface. For this research, SEM-EDX model JEOL-JSM 5410 and EDX Oxford ISIS-Link have been used.

3.4. Electrochemical Performance. Operation and Polarization VI Curve

To carry out the last stage, each membrane subjected to the exposed protocols, is put into a single-cell AEM stack that operates in a test bench, **Figure 6**. Both the stack and the test bench have been designed and developed by authors, at the research centre CITES, at the University of Huelva. The test bench is made up of the following components: 1) AEM single-cell stack, designed and developed by authors, 2) volumetric flask that contains electrolyte dissolution (0.1 M KOH), 3) electronic heater to keep the electrolyte solution at recommended temperature for electrolysis ($T = 60\,°C$), 4) peristatic pump, model Tapflo - PT10 GR-05/43, that guarantees the alkaline electrolyte recirculation, 5) power supply, model Newpower 3000 W–100 A, 6) flow controller, model ABB ACS355, to fix the electrolyte flow, 7) arduino-based controller board, model NI USB 6002, which receives the signals from sensors to monitor in real time the plant, and 8) temperature controller STC 1000 thermostat, with 220 V NTC probe to monitor the electrolyte temperature and keep it around 60 °C.

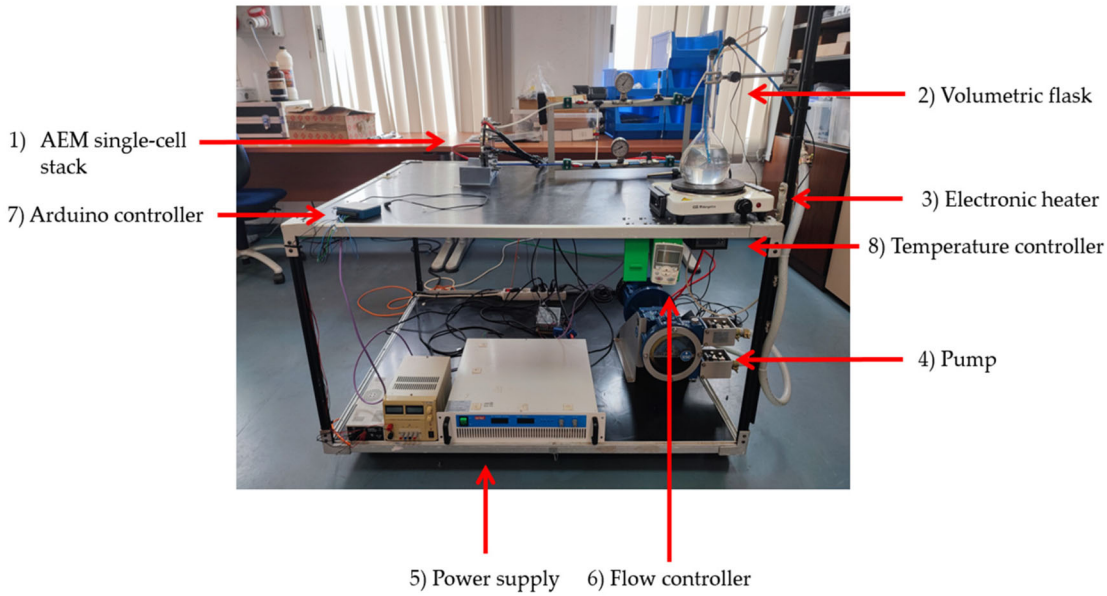

Figure 6. Test bench developed for the research.

4. Experimental Results

In this section, experimental results obtained from SEM-EDX test and polarization curves are presented and discussed by each proposed protocol.

4.1. SEM-EDX of Not Pretreated Membrane

Images obtained from SEM microscopy provided very important information about the surface of the membranes. In protocol a) *Without pretreatment* (Figure 5), the following operations have been established in the SEM. The samples have been excited with an accelerating voltage of 20 kV in high vacuum, at 9.9 mm working distance and at a magnification of 100*x*, 200*x*, and 500*x*. The surface of the samples can be observed in **Figure 7** and Appendix A,Figure A1.

At low magnification (100*x*) it can be observed that the surface of the sample is very uniform and there are few impurities. These impurities, which the SEM detector shows in a whitish colour, are particulate matter (PM) from the air that has adhered to the surface of the membranes. PM can degrade the chemical structure of the membrane's polymer backbone by promoting processes such as surface abrasion, surface soiling, and oxidative degradation. However, this phenomenon only occurs when the polymer has been exposed to PM for a prolonged period and high concentrations accumulate on its surface.[19,20] In our case, the non-pretreated membrane has only been in contact with atmospheric air for a short period (40–50 s), the minimum possible until it was introduced into the electron microscope. Therefore, the presence of PM is not a significant factor that would affect the performance of the AEM cell. Similarly, in the rest of the protocols where the membrane has been pretreated, the membrane's exposure time to atmospheric air is also minimal, so the effect of PM is not significant, and no preventive action is necessary to mitigate it. When magnification is increased (200*x*), the surface of the sample seems to be fractured. These fracture lines are not characteristic of the membrane, but have been formed by the application of the high vacuum inside the SEM. As the layer of the membrane is very thin, the membrane structure has been weakened. Finally, with the last magnification of 500*x*, the weakening of the membrane structure and the presence of PM is better observed.

Subsequently, the results obtained by X-ray (EDX) were studied. As can be seen in the EDX images, **Figure 8** and **Figure B1**, the composition of the membrane is uniform. The characteristic peaks of each element can be analysed, making the element determination unambiguous and accurate. The membrane is mainly composed of carbon (88–94%), which is the backbone of the polymer, and, in smaller percentages, there is oxygen and chlorine. The oxygen composition varies depending on the sample area studied (5–11%), however, the chlorine concentration remains unchanged at 0.2%. Chlorine is the group that is involved in the ion exchange with the hydroxyl groups during the membrane pretreatment. Therefore, by quantifying the chlorine content on the membrane surface it is possible to conclude whether the pretreatment has been effective.

4.2. SEM-EDX of a Membrane Pretreated According to Manufacturer's Protocol

In protocol b) *Manufacturer's protocol* (Figure 5) the same protocol has been applied in the SEM as in the previous case (20 kW in high vacuum, working distance of 9.9 mm and magnifications of 100*x*, 200*x*, and 500*x*), but the membrane pretreated according to the manufacturer's protocol. The results obtained are shown in Figure 7 and Appendix A, **Figure A2**. Something like the previous case is observed, due to the presence of PM as a contaminant on the membrane surface. Additionally, as magnification

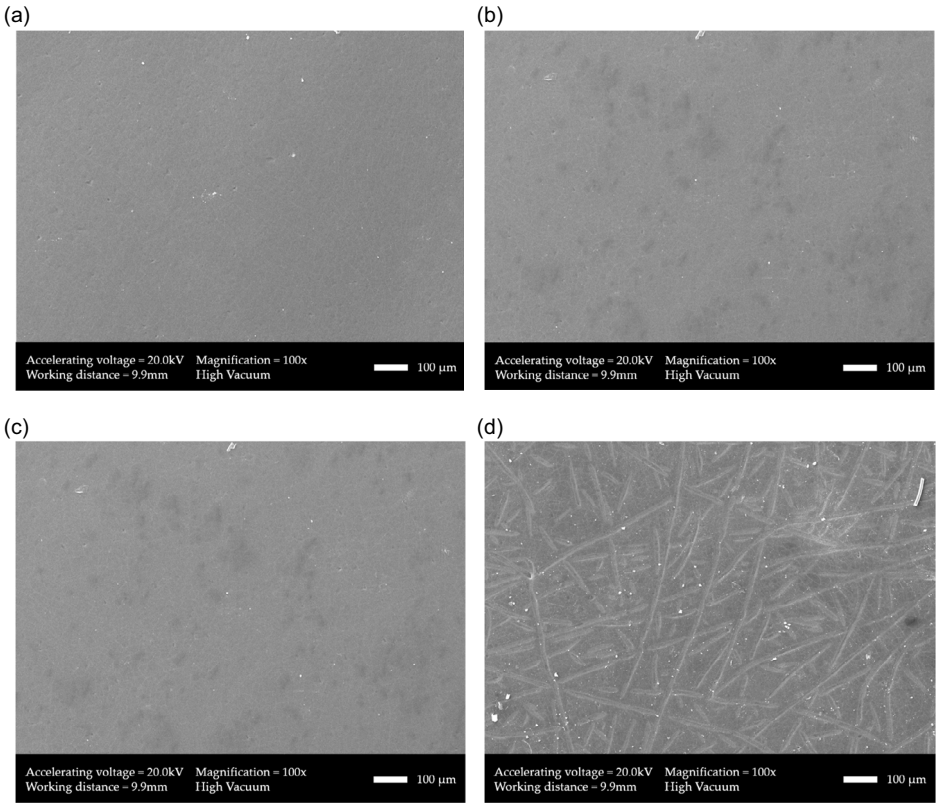

Figure 7. a) SEM analysis of non-pretreated membrane, excited with an accelerating voltage of 20 kV in high vacuum, with 100*x* magnification. See Appendix A, Figure A1 for magnifications b) 200*x* and c) 500*x*. b) SEM analysis of the membrane pretreated according to manufactured protocol, excited with an accelerating voltage of 20 kV in high vacuum with 100*x* magnification. See Appendix A, Figure A2 for magnifications b) 200*x* and c) 500*x*. c) SEM analysis of the membrane pretreated according to modified manufacturer's protocol, excited with an accelerating voltage of 20 kV in high vacuum with 100x magnification. See Appendix A, Figure A3 for magnifications b) 200 × and c) 500*x*. d) SEM analysis of the membrane pretreated according to authors' proposal protocol, excited with an accelerating voltage of 20 kV in high vacuum with 100*x* magnification. See Appendix A, Figure A4 for magnifications b) 200*x* and c) 500*x*.

increases, the membrane surface also appears to be damaged due to high vacuum conditions, although this is not significant either. A small difference that can be observed is the presence of areas with a darker colour compared to the non-pretreated membrane. These areas have formed due to the pretreatment itself, as they are marks left on the membrane by the moisture it contains. This is later confirmed in the EDX analysis.

In the EDX analysis, Figure 8 and Appendix B, **Figure B2**, a difference is observed compared to the non-pretreated membrane. In this case, the chlorine content has decreased from 0.2% to 0.1%, indicating that the pretreatment has been effective and that the ion exchange between the chloride groups of the membrane and the hydroxyl groups of the basic medium has occurred. The Tokuyama A210 membrane is composed of hydrocarbon polymer backbone with quaternary ammonium linked by electrostatic interactions with chloride ions, as mentioned earlier. If it is possible to replace many chloride ions with hydroxyl groups during the pretreatment and achieve at the same time a good level of hydration of the membrane, these processes will have already occurred prior to the application of electric current. This has several positive effects on the performance of electrolysis. Firstly, the waiting time required for the membrane to condition is shorter, because the membrane channels are already open due to hydration, so the hydroxyl groups can easily migrate from the cathode to the anode. In the same way, ion migration during electrolysis has been promoted by the prior replacement of chloride ions by hydroxyl groups, since the closer the membrane is to its fully hydroxyl-substituted form, the more ion-exchangeable sites on the membrane become active.[21–23] Secondly, by reducing the chloride ion content in the membrane, these ions will not pass to the electrolyte during electrolysis. In the case of a single membrane, no significant effect is expected, as the amount of chlorine ions is small. However, in a multi-cell medium-size electrolyser stack, the contribution of chloride ions from the membranes of each individual cell in the electrolyser presents a contamination problem, as these ions would remain in the medium.

Chloride ion substitution from 0.2% to 0.1% might seem insignificant at first glance, but it is important to remember that this process occurs at an atomic level. Therefore, this reduction, although it may appear small, is significant. If the exact amount of chlorine were to be quantified, more precise techniques, such as ICP-OES, would need to be used. However, EDX provides a general idea of how the process occurred and whether the ion-exchange process has taken place. Furthermore, as mentioned earlier, the dark areas on the membrane surface are not due to contamination or degradation during the membrane pretreatment. This is

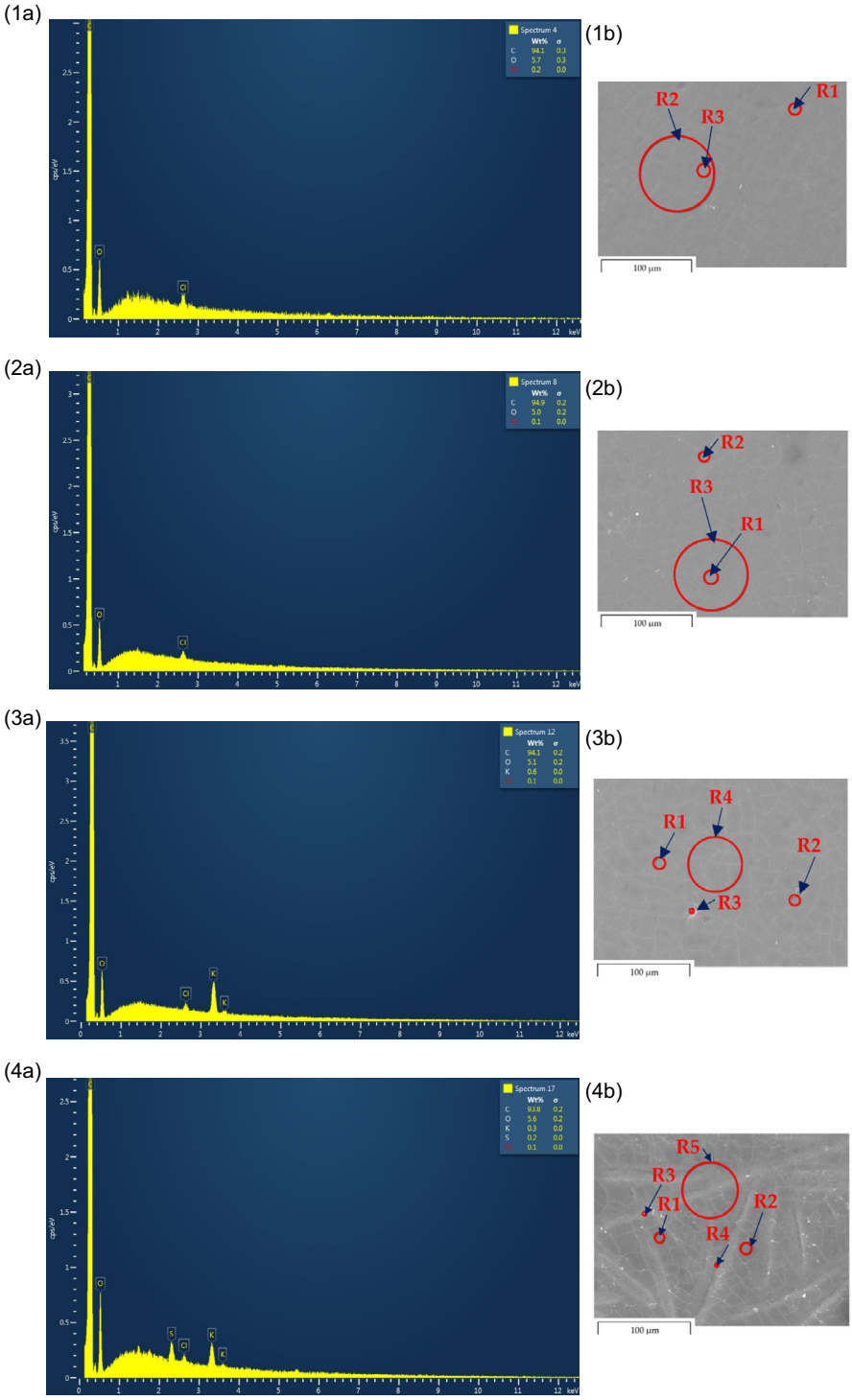

Figure 8. 1a) EDX analysis of the non-pretreated membrane, excited with an accelerating voltage of 20 kV in high vacuum, at different points of the SEM image to determine the elemental composition of the region R1. See Appendix B, Figure B1 for region R2 and R3. 1b). Regions selected for analysis (R1, R2 and R3). 2a) EDX analysis of the membrane pretreated according to manufacturer's protocol, excited with an accelerating voltage of 20 kV in high vacuum, at different points of the SEM image to determine the elemental composition of the region R1. See Appendix B, Figure B2 for region R2 and R3. 2b). Regions selected for analysis (R1, R2, and R3). 3a) EDX analysis of the membrane pretreated according to modified manufacturer's protocol, excited with an accelerating voltage of 20 kV in high vacuum at different points of the SEM image to determine the elemental composition of the region R1. See Appendix B, Figure B3 for region R2, R3, and R4. 3b). Regions selected for analysis (R1, R2, R3, and R4). 4a) EDX analysis of the membrane pretreated according to authors' protocol with an accelerating voltage of 20 kV in high vacuum a different point of the SEM image to determine the elemental composition of the region R1. See Appendix B, Figure B4 for region R2, R3, R4, and R5. 4b). Regions selected for analysis (R1, R2, R3, R4, and R5).

confirmed by studying the EDX spectrum, Figure 8 and Appendix B, Figure B2), as the composition matches (except for chlorine) with that of the non-pretreated membrane. There is a high concentration of carbon (92–94%) and oxygen content between 5 and 7%. Therefore, the presence of any type of impurity or external contaminant is ruled out, and it is accepted that these areas are marks from excess moisture.

4.3. SEM-EDX of a Membrane Pretreated According to Modified Manufacturer's Protocol

For the SEM analysis, the same procedure as in the previous case was carried out (20 kW in high vacuum, working distance of 9.9 mm and magnifications of 100*x*, 200*x*, and 500*x*), but for the membrane pretreated according to protocol c) *Modified manufacturer's protocol* (Figure 5). The results obtained are shown in Figure 7 and Appendix A, **Figure A3**. The SEM analysis does not show any significant difference compared to the previous case, as there is again the presence of contamination by atmospheric PM. When the magnification is increased (200*x*), the presence of fracture lines is observed, and there are areas with a darker color due to the moisture in the sample. The real difference of applying this pretreatment is not visible by analysing only the SEM results; one must also refer to the EDX results to understand which is the difference between the pretreatment techniques employed. This pretreatment technique differs from the one proposed by the manufacturer in the time the membrane is immersed in the KOH solution (20 min instead of 30 min) and in the final stage. In the case of the manufacturer's protocol, the pretreated membrane is cleaned with distilled water, whereas, in the modified protocol, this step is not followed.

When analysing the images obtained by EDX, Figure 8 and Appendix B, **Figure B3**, it can be observed that, in addition to carbon, oxygen, and chlorine, there is an additional element: potassium. The concentration of potassium is not very high (0.6–0.7%), but it indicates that if the membrane is not cleaned with Milli-Q water after pretreatment, potassium remains on its surface. The presence of potassium has a positive effect on the surface conductivity of the membrane. Surface conductivity describes the enhanced electrical conduction occurring at solid–liquid interface, driven by the movement of excess ions in response to electric fields. This phenomenon is measured using a one-dimensional conduction parameter (κ^{σ}), which is influenced by the concentration and mobility of ions within the interfacial region.[24,25] Therefore, although the potassium concentration on the surface of the membrane that has not been cleaned with Milli-Q water is not very high, these ions improve the surface conductivity of the membrane during the initial stages of electrolysis compared to the previous protocol. As it will be demonstrated in section 4.4, even if the membrane is conditioned inside the stack, in the test bench, for 8 h to continue loading it with potassium and increasing its surface conductivity, it does not absorb more potassium on its surface. Thus, this pretreatment protocol decreases the time needed for the membrane to reach its maximum surface conductivity due to the action of potassium. The concern would be if this process affects the chlorine present in any way. However, the same result as in the previous case has been obtained, as the chlorine concentration is around 0.1%, meaning the exchange has also occurred correctly. The chlorine concentration has decreased to 0.1% as in the previous case because both techniques are similar, so a large difference between the results was not expected. It was only expected that not cleaning the membrane with water would increase the initial surface conductivity of the membrane.

4.4. SEM-EDX of a Membrane Pretreated and Conditioned According to Authors' Proposal Protocol

For the SEM analysis, the same procedure as in the previous case was carried out (20 kW in high vacuum, working distance of 9.9 mm and magnifications of 100*x*, 200*x*, and 500*x*), but for the membrane pretreated according to protocol d) *Authors' proposal* (Figure 5). In this protocol, the conditioning phase of 8 h operating in the test bench is of great interest not only to analyse the chlorine substitution but also to see how the membrane behaves inside the stack. The results obtained are shown in Figure 7 and Appendix A, **Figure A4**.

The SEM images show a major difference from previous analyses. Firstly, in addition to the PM present on the surface of the membrane, the presence of impurities can also be seen. This can be seen more closely when the magnification is increased (500*x*). In addition to the contamination of the membrane, a series of marks can be seen very clearly, which are not the fracture lines mentioned earlier, but they are marks generated on the surface of the membrane when it is assembled in the electrolytic stack. However, the structural strength of the membrane was not compromised, as the membrane was still performing its function and there was no short-circuit in the system during the tests. These marks are best observed at low magnification (100*x*).

Analysis of the EDX images proved the aforementioned assumptions to be true, Figure 8 and Appendix B, **Figure B4**). Firstly, it should be noted that following the authors' protocol, chlorine substitution up to 0.1% also occurs, so the methodology followed is adequate. Secondly, the presence of potassium in the membrane is observed as in the previous pretreatment protocol. However, this is due to the 8-hour conditioning, as the pretreatment with Milli-Q water cannot supply these ions. Besides, Figure 8 shows the presence of S, while Figure B4 shows a large variety of metallic elements (Ti, Fe, Cr, and Al) in addition to S, Si, and Cs. These impurities are due to the metal components of the test bench. As the electrolyte is recirculated through the system, these components release metal particles and impurities that are deposited on the membrane. For short operating times, this is not a problem, but for long duration tests it can significantly affect the performance of the membrane and promotes its chemical degradation. This accumulation of metallic particles is not related to the pretreatment applied. Authors are working on a future work focused on optimisation of the components in the test bench, degradation tests and chronopotentiometries.

4.5. Electrochemical Analysis: Operation and Polarization Curve

As a complement to this study, a set of tests was carried out to corroborate the previous analysis with experimental data. Using the test bench designed by authors (Figure 6), the membranes have been putting into operation, integrating into a single-cell stack,

and testing the performance of the four described pretreatment protocols (without pretreatment, manufacturer's protocol, modified manufacturer's protocol, and authors' proposal). The objective is to check whether significant changes in current density values occur when applying the protocols shown in Figure 5. As can be seen in **Figure 9**, there are differences in electrochemical behaviour, according to polarization curve, voltage versus current density.

The best results are obtained from the authors' proposal (green line), since for the same voltage the current density obtained is higher due to a better opening of the membrane channels by hydrating the membrane for 7 days and a good ion exchange achieved in the 8-hour conditioning. On the contrary, the manufacturer's protocol and modified manufacturer's protocol are worse options (red and black line, respectively), but they are also an improvement compared to membrane which is not pretreated (blue line). As mentioned earlier, the modified manufacturer's protocol should be better than the manufacturer's protocol, since the membrane was not cleaned with Milli-Q water and potassium remains on its surface, so it has better initial surface conductivity. Therefore, the losses in the activation part are reduced, resulting in a higher current density at low voltage.

To quantitatively interpret the results shown in Figure 9, a calculation will be made to determine the efficiency of the AEM electrolytic stack and to be able to compare based on numerical data. The efficiency of a stack can be determined with reasonable accuracy by applying Faraday's law (1) and equation (2). This calculation assumes that the amount of current consumed is directly proportional to the amount of hydrogen produced. The relationship is described as:

$$m = \frac{M \cdot Q}{z \cdot F} \tag{1}$$

where:
m: mass of the substance produced (g)
M: molar mass of the substance produced (2 g·mol^{-1} for H_2)
Q: electric charge passing through the stack (C)
F: Faraday constant (96485.33 C mol^{-1})
z: valence number of the produced substance (2 for H_2)
The charge Q can be expressed as:

$$Q = I \cdot t \tag{2}$$

where:
I: electric current intensity (A)
t: elapsed time (s)
By substituting (2) into (1):

$$m_{H_2} = \frac{M \cdot I \cdot t}{z \cdot F} \tag{3}$$

This demonstrates that hydrogen production is proportional to the current applied to the stack over time. Hydrogen produced also has associated energy, which depends on its calorific value. For most practical purposes, the lower calorific value (LHV) of hydrogen is used, as it represents the usable energy. The energy of the produced hydrogen is calculated as:

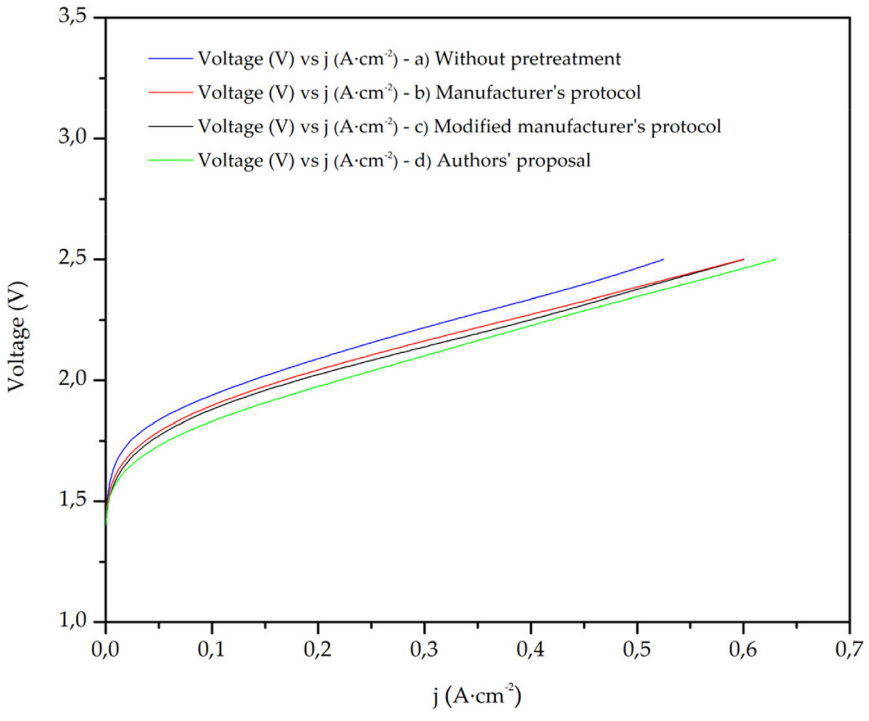

Figure 9. Comparative study of polarization curve, voltage (V) versus current density (mA·cm^{-2}) from each pretreatment protocol: a) Without pretreatment, b) Manufacturer's protocol, c) Modified manufacturer's protocol and d) Authors' proposal protocol. Test conditions: Tightening torque = 10 N·m, electrolyte flow rate (KOH 0.1 M) = 0.1 L/min, cathode nickel foam diameter = 90 mm, anode nickel foam diameter = 100 mm, foams thickness = 3 mm, foam porosity = 90 PPI, temperature = 60 °C, oxygen and water recirculation in independent compartments.

$$E_{H_2} = m_{H_2} \cdot \ LHV_{H_2} \quad (4)$$

where:

E_{H_2}: Hydrogen energy (Wh)

LHV_{H_2}: Hydrogen lower heating value (33.33 $Wh \cdot g^{-1}$)

By combining Equation (3) and (4), the energy produced in form of hydrogen can be expressed as (5).

$$E_{H_2} = \frac{M \ \cdot \ LHV_{H_2} \cdot I \cdot t}{z \ \cdot \ F} \quad (5)$$

And the electrical energy consumed by the single-cell electrolytic stack is calculated in (6).

$$E_{consumption} = V \ \cdot I \ \cdot \ t \quad (6)$$

where:

$E_{consumption}$: Electrical energy consumed by the electrolytic stack (Wh)

V: Cell voltage (V)

The faraday's efficiency $\eta_{Faraday}$ is defined as the ratio of energy obtained from hydrogen production to the energy input, which can be expressed as:

$$\eta_{Faraday} = \frac{E_{H_2}}{E_{consumption}} = \frac{\frac{M \cdot LHV_{H_2} \cdot I \cdot t}{z \cdot F}}{V \ \cdot I \ \cdot \ t} = \frac{M \ \cdot \ LHV_{H_2}}{V \ \cdot z \ \cdot \ F} \quad (7)$$

Thus, the Faradaic efficiency of the stack depends on constants and the operating cell voltage. For a given current density, the efficiency can be determined using the stack's polarization curve. Therefore, the performance of the AEM electrolytic single-cell stack will be calculated for a given current value (500 $mA \cdot cm^{-2}$) using the different voltage values that have been necessary to reach this current density. In this way, the quantitative improvement in efficiency of each pretreatment technique can be determined compared to the non-pretreated membrane. Equation (8) gives the general expression for calculating the efficiency for pretreatment protocol

$$\eta_{Faraday_{500\ \frac{mA}{cm^2}}} = \frac{2\ \frac{g}{mol} \ \cdot \ 33.33\ \frac{Wh}{g} \cdot \ 3600\ \frac{s}{h}}{V_{500\ \frac{mA}{cm^2}} \cdot \ 2 \ \cdot \ 96485.33\ \frac{C}{mol}} \ \cdot \ 100\% \quad (8)$$

Applying Equation (8) for the different pretreatment protocols, it is quantitatively concluded that the best performance is obtained from authors' proposal (**Table 4**).

Table 4. Efficiency of the electrolyser applying the different pretreatment techniques.

Pretreatment protocol	Density current [$mA \cdot cm^{-2}$]	Cell voltage [V]	$\eta_{Faraday_{500\ \frac{mA}{cm^2}}}$ [%]
(a) Without pretreatment	500	2.46	50.55
(b) Manufacturer's protocol	500	2.38	52.25
(c) Modified manufacturer's protocol	500	2.36	52.69
(d) Authors' proposal	500	2.34	53.14

Considering the results obtained (Table 4), applying the authors' pretreatment and conditioning technique increases the efficiency of the stack by ≈2.6% ($\eta_{Faraday(a)} - \eta_{Faraday(d)} = 53.14–50.55\%$).

4.6. Tafel Slope and Ohmic Resistance Analysis

The Tafel equation allows to relate the overpotential of an electrode and the rate of the electrochemical reaction. This type of representation is used to study electrochemical reaction mechanisms, relating these processes to the overpotential value necessary for the reaction to occur.[26–28] The Tafel equation for evaluating the effect of overpotential and current density is given below

$$\eta = \pm A \cdot \log(j/j_o) \quad (9)$$

where:

η: Overpotential (V)

A: Tafel slope ($V \cdot dec^{-1}$)

j: Density current ($mA \cdot cm^{-2}$)

j_o: Exchange current density ($mA \cdot cm^{-2}$)

The overpotential is calculated by subtracting the voltage applied to the system minus the theoretical decomposition voltage of water in an electrolytic cell (1.23 V). The constant j_o is related to the surface properties of the electrode, while the constant A is the Tafel slope and j is the current density in $mA\,cm^{-2}$. All values except A and j_o are known, so the above expression (9) is readjusted to determine them from the graphical representation of the overpotential values and the logarithm of the current density.

$$\eta = A \cdot \ [\log(j) - \log(j_o)] \quad (10)$$

$$\eta = A \cdot \ \log(j) - A \cdot \ \log(j_o) \quad (11)$$

Considering the expression (10), since all the voltage and current density values are given, the Tafel slope ($V \cdot dec^{-1}$) and the exchange density current ($mA \cdot cm^{-2}$) can be calculated for each value. In this way, the slope values for each protocol can be compared and conclusions can be drawn. The values obtained for each voltage are compiled in **Table 5** and plotted in **Figure 10** and **Figure C**.

Once the overpotential has been plotted against the logarithm of the current density for each pretreatment protocol, it is concluded that the protocol proposed by the author represents an improvement with respect to the non-pretreated membrane. In the electrochemical process, the activation part of the membrane and the ohmic losses come into play. As can be seen in Table 5, although the Tafel slope for the protocol proposed by the author is slightly higher than the case in which the membrane was not pretreated, as

Table 5. Tafel slope a ($V \cdot dec^{-1}$), exchange current density j_0 ($mA \cdot cm^{-2}$) and its ratio.

Pretreatment protocol	j_0 [$mA \cdot cm^{-2}$]	A [$V \cdot dec^{-1}$]	A/j_0 [$V \cdot cm^2 \cdot mA^{-1} \cdot dec^{-1}$]
(a) Without pretreatment	92.61	1.69	0.018
(b) Manufacturer's protocol	112.91	1.77	0.016
(c) Modified manufacturer's protocol	126.90	1.90	0.015
(d) Authors' proposal	158.07	2.14	0.014

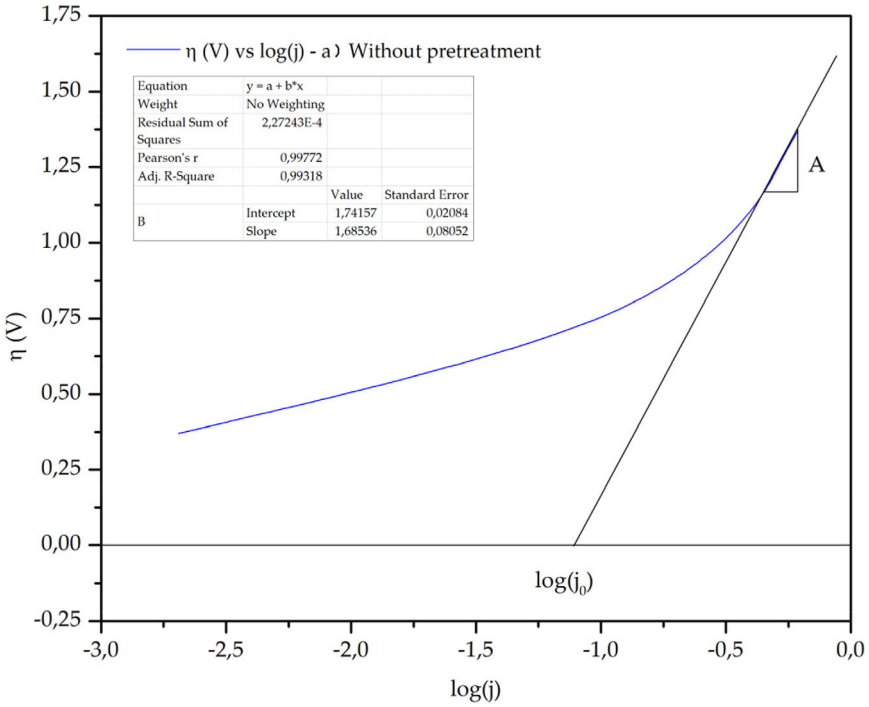

Figure 10. Representation of overpotential (η) versus the logarithm of density current (j) to determine the Tafel slope of the anode compartment of the electrolyser: a) Without pretreatment. See Appendix C, Figure C for see the curve obtained in the cases: b) Manufacturer's protocol, c) Modified manufacturer's protocol, and d) Authors' proposal protocol.

the exchange current density is higher for the author's case, the ratio between both parameters is smaller. Therefore, considering the activation and ohmic effect, a lower overvoltage is necessary to reach the same current density value.

5. Discussion

Based on obtained results, we can observe that the efficiency improvement by applying the authors' protocol is 2.6%. This result can be compared with other scientific works focused on other key aspects of electrolysis performance, such as operating conditions or the electrocatalytic part of the reaction.[29–32] The efficiency improvement obtained from authors' proposal is interesting because there are no references to previous studies by other researchers focused on optimising AEM membrane pretreatment protocols. Normally, AEM electrolysis studies downplay the importance of the pretreatment conditions, which results in generic descriptions of the protocols without focusing on them.[5,33] It has been demonstrated that the 2.6% gain in efficiency when the membrane is pretreated using author's protocol, is due to the opening of the polymer channels when the membrane is properly hydrated for 7 days (increasing ion conductivity). A higher surface conductivity due to the accumulation of potassium on the membrane surface and a higher substitution ratio of hydroxyl groups during the 8 h conditioning, generates active sites that promote the migration of ions between the cathode and the anode. All these points optimise the performance of the membrane and help to make its useful life more efficient and long-lasting.

On the contrary, the protocol proposed by authors guarantees raw material savings (KOH and water), with all the environmental benefits this entails. The main novelty of this research article compared to other studies is that it presents an alternative pretreatment protocol that does not use KOH solutions, reducing the use of reagents and waste generation. These improvements are in accordance with Sustainable Development Goal 12 (SDG 12: Responsible Consumption and Production). One of the key aspects of SDG 12 focuses on reducing the use of raw materials and improving energy efficiency in industrial processes, making the authors' proposal align with this objective.[34] To quantify the waste reduction achieved by authors protocol, it is necessary to consider the amount of KOH and Milli-Q water used when the membrane was pretreated following both the manufacturer's protocol and the modified manufacturer's protocol. In both protocols, 6.17 g of KOH/membrane (Alquera, p.a = 90%) was mixed with 1 L of Milli-Q water/membrane. One-liter solution was prepared to fully immerse the membrane in the medium and to ensure that the hydration occurs correctly. Depending on the active area and the application of the electrolyser, the number of cells and thus the number of membranes to achieve a certain power varies. Taking as reference the operating point at 500 $mA{\cdot}cm^{-2}$ and 2.34 V, Table 4, considering an active area of 63.61 cm^2/cell, the electrical power requirement is 74.43 W/cell. Then, a 1 kW-electrolyser would require about 14 cells. Then, the authors pretreatment protocol will allow to save 86.34 g of KOH/kWe (6.17 g/membrane, 14 membranes) and 14 L of water/kWe (1 L/membrane, 14 membranes). It is also important to consider that water contaminated with KOH would have to undergo post-treatment to be reused or discharged into the environment, so this is another additional energy cost that has been saved.

6. Conclusions

This work has presented a comprehensive study focused on analysing the effects of pretreatment on ion-exchange membranes used in AEM electrolysis technology. For this study, the research has carried out a comparative regarding morphology and surface composition of the membranes. The methodology involves four stages: laser cutting, pretreatment protocols definition, SEM-EDX image capture and operation, and polarization curve comparison.

The main novelties of this work are: 1) the protocol proposed by authors, which guarantees raw material saving, and 2) this research integrates both morphological and electrical performance analyses to evaluate the pretreated membranes, considering not only their chemical composition but also their interaction with the complete electrolysis plant. Obtained results demonstrate how pretreatment techniques affect membranes, correlating morphological modifications with their electrochemical performance. In particular, the specific conclusions obtained from the research are: 1) The non-pretreated membranes have a chlorine content of 0.2%, which can be halved by using the various pretreatment techniques studied; 2) Although the chlorine content is low and consequently its substitution is low, it is sufficient to facilitate the exchange of hydroxyl groups during the operation of the AEM stack; 3) As for the pretreatment techniques used, the protocol proposed by authors leaves potassium on the surface of the membranes and allows an adequate chlorine substitution (from 0.2% to 0.1%), which increases their surface and ionic conductivity, respectively. This has been corroborated experimentally with the study of polarization curve values; 4) The pretreatment protocol is key in the AEM electrolysis efficiency. It has been demonstrated that not pretreating means lower efficiency. By contrast, the protocol proposed by authors, based on immersing for 7 days the membrane directly in Milli-Q water, avoiding the waste of KOH solution, and putting it into operation for 8 days to guarantee the ion-exchange process, offers the best performance, improving the efficiency in 2.6% with respect the efficiency obtained from manufacturer's protocol; 5) The pretreatment protocol proposed by authors has a lower ratio between Tafel slope and exchange current density, which is an indication that a lower amount of overvoltage is needed to achieve the same current density value; 6) For future research, authors are working on continued tests with membranes pretreated longer, membrane conditioning tests on the long-term and chronopotentiometry monitoring. In this way, it would be possible to see how much more hydrogen production efficiency can be improved by optimising the performance AEM membranes.

Appendix A

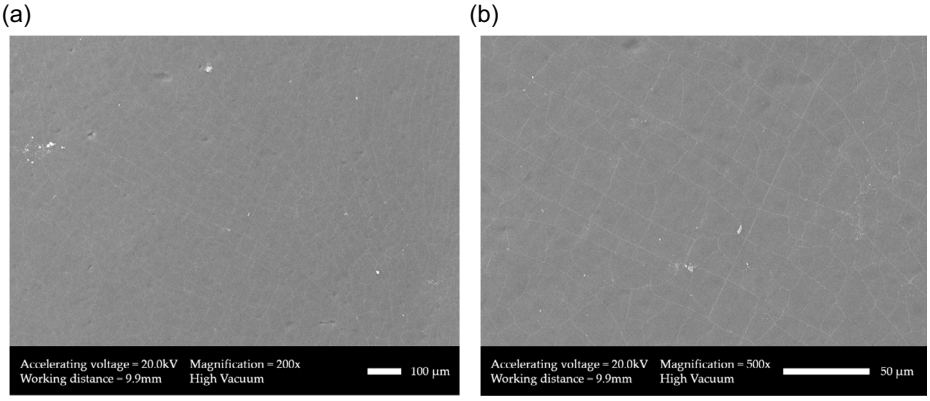

Figure A1. SEM analysis of the non-pretreated membrane, excited with an accelerating voltage of 20 kV in high vacuum, with different magnifications: a) 200*x* and b) 500*x*.

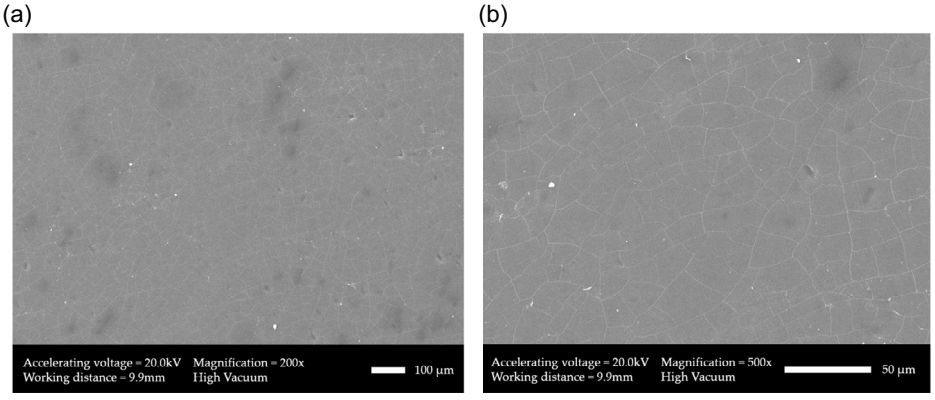

Figure A2. SEM analysis of the membrane pretreated according to manufacturer's protocol, excited with an accelerating voltage of 20 kV in high vacuum with different magnifications. a) 200*x* and b) 500*x*.

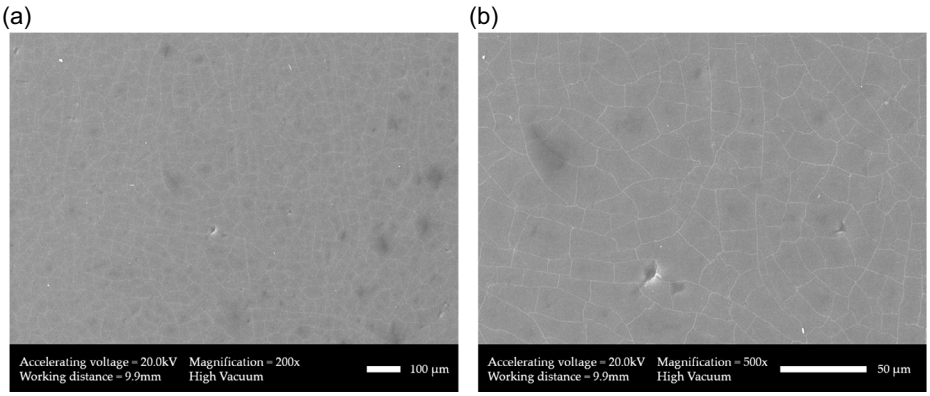

Figure A3. SEM analysis of the membrane pretreated according to modified manufacturer's protocol, excited with an accelerating voltage of 20 kV in high vacuum with different magnifications: a) 200*x* and b) 500*x*.

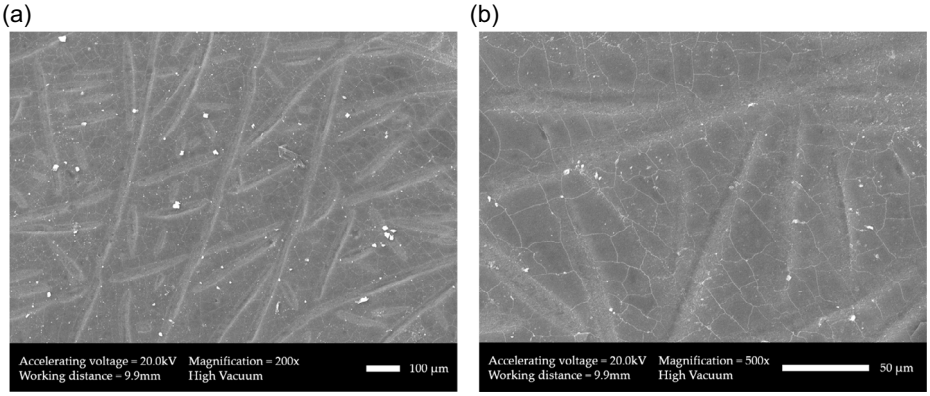

Figure A4. SEM analysis of the membrane pretreated according to authors' proposal protocol, excited with an accelerating voltage of 20 kV in high vacuum with different magnifications. a) 200*x* and b) 500*x*.

Appendix B

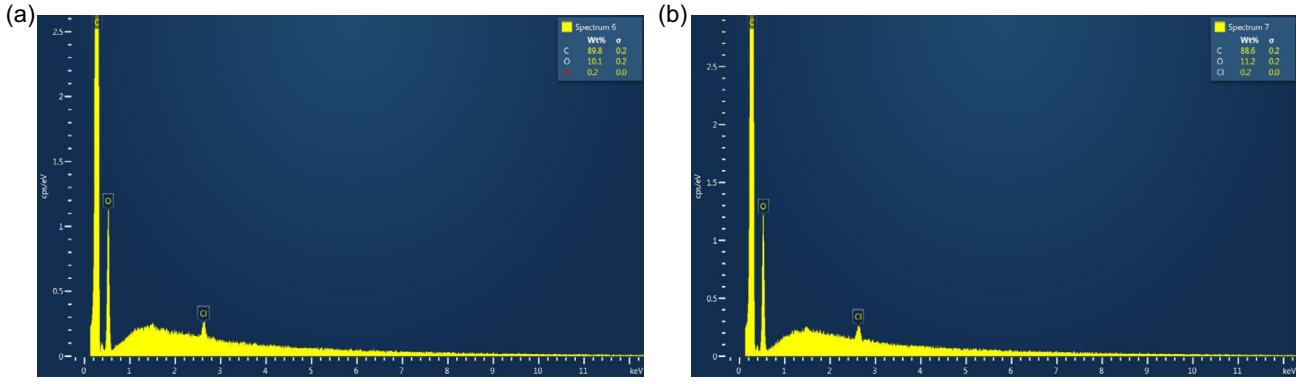

Figure B1. EDX analysis of the non-pretreated membrane, excited with an accelerating voltage of 20 kV in high vacuum, at different points of the SEM image to determine the elemental composition. (a) Region R2 - (b) Region R3.

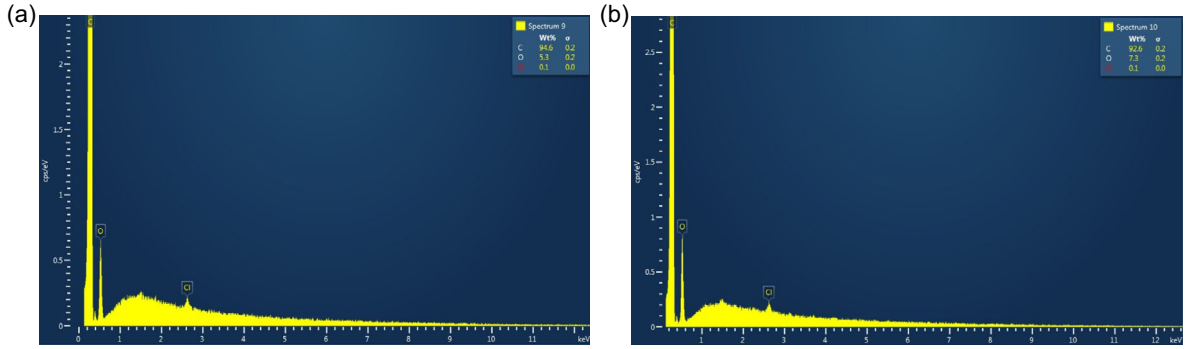

Figure B2. EDX analysis of the membrane pretreated according to manufacturer's protocol, excited with an accelerating voltage of 20 kV in high vacuum, at different points of the SEM image to determine the elemental composition. (a) Region R2 - (b) Region R2.

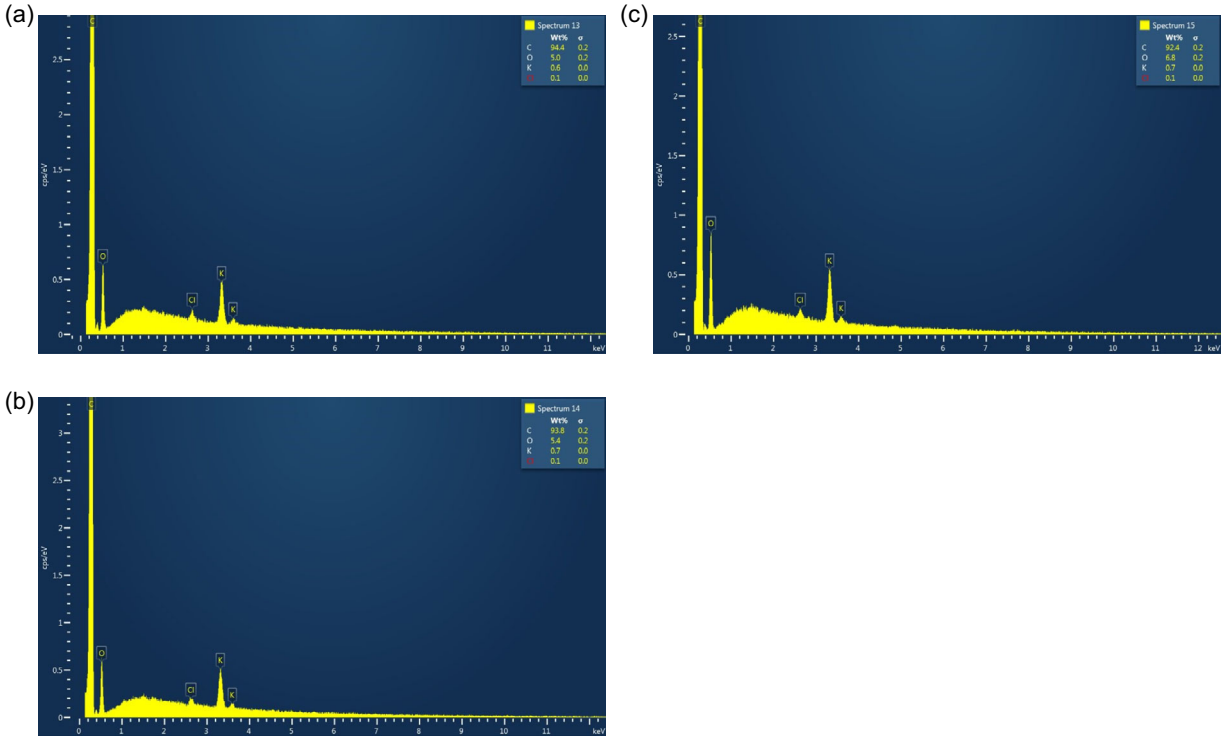

Figure B3. EDX analysis of the membrane pretreated according to modified manufacturer's protocol, excited with an accelerating voltage of 20 kV in high vacuum at different points of the SEM image to determine the elemental composition. (a) Region R2, (b) Region R3, (c) Region R4.

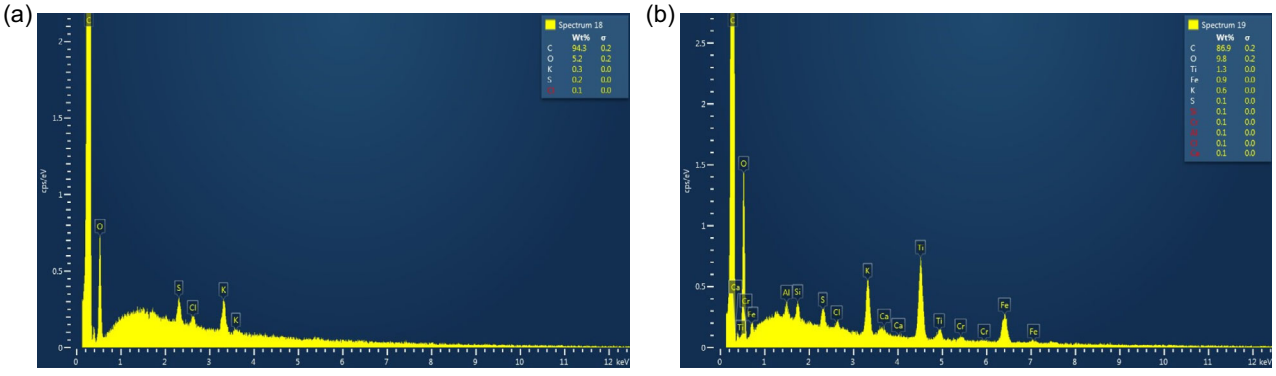

Figure B4. EDX analysis of the membrane pretreated according to authors' protocol d) with an accelerating voltage of 20 kV in high vacuum a different point of the SEM image to determine the elemental composition. (a) Region R2, (b) Region R3, (c) Region R4, and (d) Region R5.

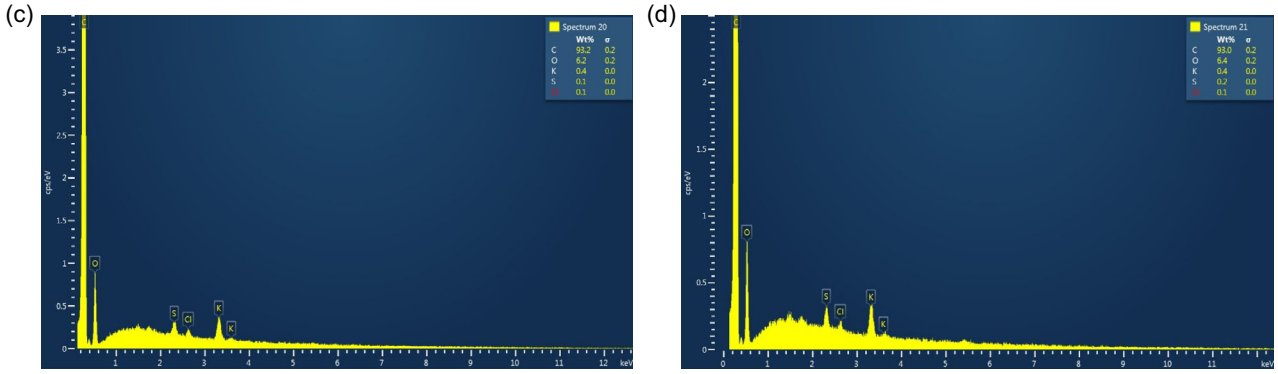

Figure B4. Continued.

Appendix C

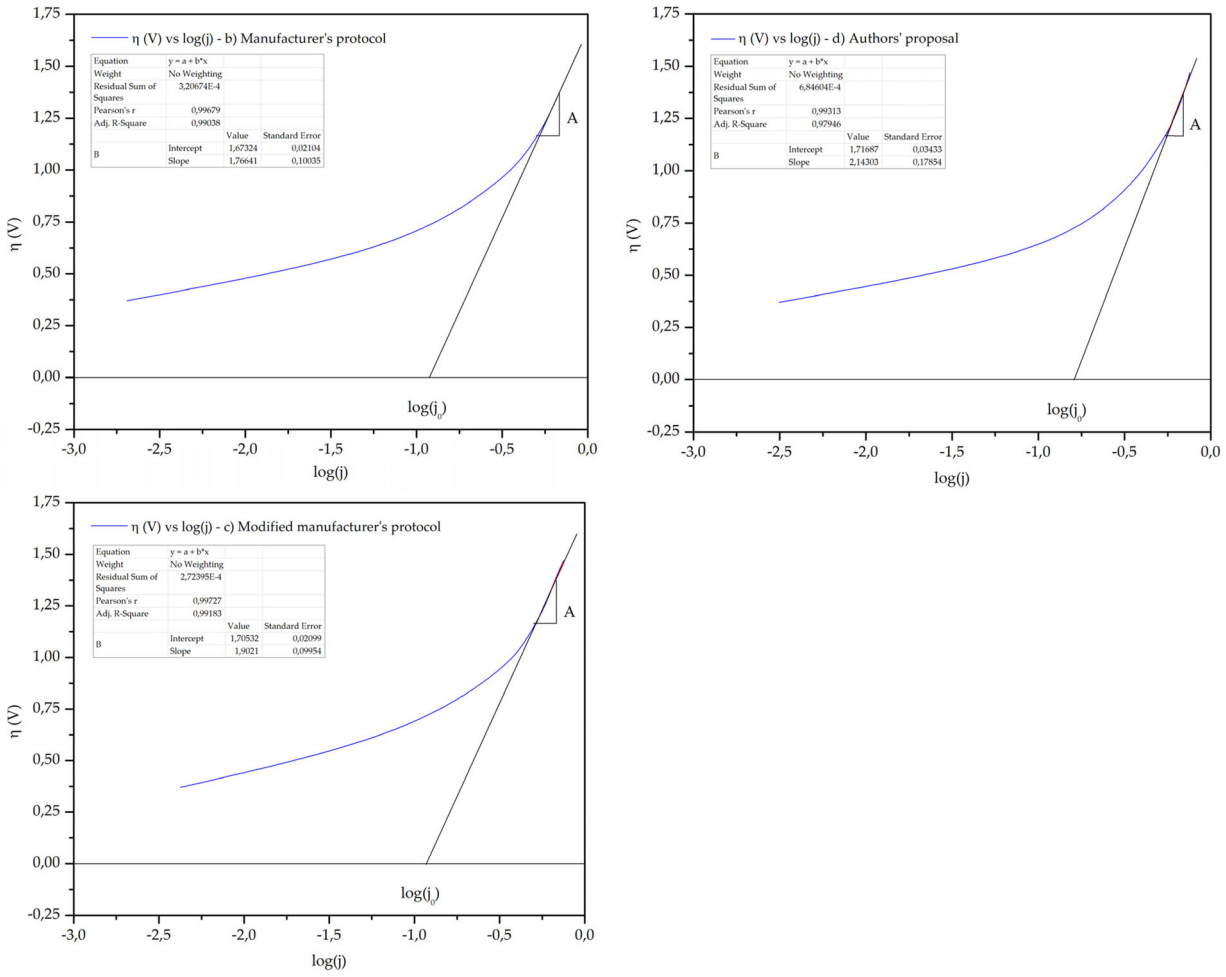

Figure C. Representation of overpotential (η) vs the logarithm of density current (j) to determine the Tafel slope of the anode compartment of the electrolyser: Protocol b) Manufacturer's protocol; Protocol c) Modified manufacturer's protocol, and Protocol d) Authors' proposal protocol.

Acknowledgements

Spanish Government Project Ref. PID2023-148456OB-C41 by MICIU/AEI/10.13039/501100011033, - Spanish Government Project Ref. RED2022-134588-T by MICIU/AEI /10.13039/501100011033.

Conflict of Interest

The authors declare no conflict of interest.

Data Availability Statement

The data that support the findings of this study are available from the corresponding author upon reasonable request.

Keywords

anion exchange membrane (AEM) electrolysis, cell polarization curve, experimental testing, membrane pretreatment, SEM-EDX analysis

Received: February 10, 2025
Revised: April 20, 2025
Published online:

[1] D. Henkensmeier, M. Najibah, C. Harms, J. Žitka, J. Hnát, K. Bouzek, *J. Electrochem. Energy Convers. Storage* **2021**, *18*, 020801.
[2] Y. Sugawara, S. Sankar, S. Miyanishi, R. Illathvalappil, P. K. Gangadharan, H. Kuroki, G. M. Anilkumar, T. Yamaguchi, *J. Chem. Eng. Jpn.* **2023**, *56*, 1.
[3] I. Vincent, D. Bessarabov, *Renewable Sustainable Energy Rev.* **2018**, *81*, 1690.
[4] G. A. Lindquist, S. Z. Oener, R. Krivina, A. R. Motz, A. Keane, C. Capuano, K. E. Ayers, S. W. Boettcher, *ACS Appl. Mater. Interfaces* **2021**, *13*, 51917.
[5] I. V. Pushkareva, A. S. Pushkarev, S. A. Grigoriev, P. Modisha, D. G. Bessarabov, *Int. J. Hydrogen Energy* **2020**, *45*, 26070.
[6] D. Xu, M. B. Stevens, M. R. Cosby, S. Z. Oener, A. M. Smith, L. J. Enman, K. E. Ayers, C. B. Capuano, J. N. Renner, N. Danilovic, Y. Li, H. Wang, Q. Zhang, S. W. Boettcher, *ACS Catal.* **2019**, *9*, 7.
[7] J. Liu, Z. Kang, D. Li, M. Pak, S. M. Alia, C. Fujimoto, G. Bender, Y. S. Kim, A. Z. Weber, *J. Electrochem. Soc.* **2021**, *168*, 054522.
[8] H. Gao, C. Jin, X. Li, Y. M. So, Y. Pan, *Polymers* **2024**, *16*, 11464.
[9] Z. Zakaria, S. K. Kamarudin, *Int. J. Energy Res.* **2021**, *45*, 18337.
[10] H. Ito, N. Miyazaki, S. Sugiyama, M. Ishida, Y. Nakamura, S. Iwasaki, Y. Hasegawa, A. Nakano, *J. Appl. Electrochem.* **2018**, *48*, 305.
[11] H. Ito, N. Kawaguchi, S. Someya, T. Munakata, N. Miyazaki, M. Ishida, A. Nakano, *Int. J. Hydrogen Energy* **2018**, *43*, 17030.
[12] K. Rouwenhorst, In *Renewable Ammonia: Technologies, Applications, and Sustainability*, Royal Society of Chemistry, London, UK **2020**, pp. 180–210. https://doi.org/10.1039/9781788016049-00180.
[13] D. Henkensmeier, M. Najibah, C. Harms, J. Žitka, J. Hnát, K. Bouzek, *J. Electrochem. Energy Convers. Storage* **2021**, *18*, 2.
[14] G. H. A. Wijaya, K. S. Im, S. Y. Nam, *Desalin. Water Treat.* **2024**, *320*, 100605.
[15] I. Vincent, A. Kruger, D. Bessarabov, *Int. J. Electrochem. Sci.* **2018**, *13*, 11347.
[16] *Electrochemical Methods for Hydrogen Production* (Ed: K. Scott), The Royal Society of Chemistry, London, UK **2019**. https://doi.org/10.1039/9781788016049.
[17] D. Hua, J. Huang, E. Fabbri, M. Rafique, B. Song, *ChemElectroChem* **2023**, *10*, 1.
[18] K. F. L. Hagesteijn, S. Jiang, B. P. Ladewig, *J. Mater. Sci.* **2018**, *53*, 11131.
[19] I. Cook, *ICCM Bull.* **1976**, *2*, 4.
[20] S. N. Kazi, *Water-Formed Deposits: Fundamentals and Mitigation Strategies*, Elsevier, San Diego, California, EE. UU **2022**, pp. 97–140. https://doi.org/10.1016/B978-0-12-822896-8.00012-1.
[21] G. Herry, A. Wijaya, K. S. Im, S. Y. Nam, *Desalin. Water Treat.* **2024**, *320*, 100605.
[22] Q. Duan, S. Ge, C.-Y. Wang, *J. Power Sources* **2013**, *243*, 773.
[23] A. Zhegur-Khais, F. Kubannek, U. Krewer, D. R. Dekel, *J. Membr. Sci.* **2020**, *612*, 118461.
[24] *Fundamentals of Interface and Colloid Science*, Academic Press, London, UK Vol. *2*, **1995**, p. 4. https://doi.org/10.1016/S1874-5679(06)80007-3.
[25] A. S. Dukhin , P. J. Goetz, Electroacoustic Theory. *Stud. Interface Sci.* **2010**, *24*, 187.
[26] O. Van der Heijden, S. Park, R. E. Vos, J. J. Eggebeen, T. M. Koper, *ACS Energy Lett.* **2024**, *9*, 1871.
[27] M. Wand, Z. Wang, X. Gong, Z. Guo, *Renewable Sustainable Energy Rev.* **2014**, *29*, 573.
[28] E. Katz, *Electrochemical Science Adv.* **2022**, *2*, 2.
[29] A. M. I. Noor Azam, T. Ragunathan, N. N. Zulkefli, M. S. Masdar, E. H. Majlan, R. Mohamad Yunus, N. S. Shamsul, T. Husaini, S. N. A. Shaffee, *Polymers* **2023**, *15*, 5.
[30] C. Li, J. B. Baek, *Nano Energy* **2021**, *87*, 106162.
[31] A. Y. Faid, L. Xie, A. O. Barnett, F. Seland, D. Kirk, S. Sunde, *Int. J. Hydrogen Energy* **2020**, *45*, 28272.
[32] A. Loh, X. Li, S. Sluijter, P. Shirvanian, Q. Lai, Y. Liang, *Hydrogen* **2023**, *4*, 257.
[33] Q. Xu, L. Zhang, J. Zhang, J. Wang, Y. Hu, H. Jiang, C. Li, *EnergyChem* **2022**, *4*, 100087.
[34] United Nations. Goal 12: Ensure Sustainable Consumption and Production Patterns. United Nations Sustainable Development Goals. **2024**. https://sdgs.un.org/goals/goal12.